http://dx.doi.org/10.15576/GLL/2021.4.147

GLL

Geomatics, Landmanagement and Landscape No. 4 • 2021, 147–167

ROBUST VEGETATION DETECTION USING RGB COLOUR COMPOSITES AND ISOCLUST CLASSIFICATION OF THE LANDSAT TM IMAGE

Polina Lemenkova

Summary

The paper presents the application of ArcGIS for environmental modelling of the landscapes in northern Iceland (17.00°W–23.00°W, 64.30°N–67.00°N). The aim was to explore the vegetation distribution by NDVI and ISOCLUST classification of the land cover types. Data include the Landsat TM image. Freely available satellite remote sensing data from the Landsat mission have been processed by GIS to deliver information on land cover types from image classification and NDVI vegetation index. Landsat products provide geospatial data on regional scale with moderate temporal (weekly) and spatial (30–10 m) resolution, making them useful for environmental monitoring and landscape studies. The tools include the ArcGIS software used for raster processing. Data processing was performed in the three steps: 1) comparative analysis of the visualized sixteen band combinations to assess the distinguishability of vegetation and other land cover types in colour composites; 2) computed NDVI standardized vegetation index; 3) unsupervised classification of the Landsat TM by the ISOCLUST algorithm. Large glaciers Hofsjökull and Langjökull were detected on various colour composites, and the visibility of the water/land borders is assessed (Blöndulón lake), agricultural areas near the Varmahlíð, vegetated areas around the Akrahreppur municipality. Computing the NDVI and using ISOCLUST by ArcGIS software enabled to distinguish various land cover types and map landscapes in the study area. The computed NDVI shown the presence and condition of vegetation, that is, a relative biomass in the area of northern Iceland. The NDVI was used based on the contrast of the two channels from a multispectral Landsat TM raster data.

Keywords

cartography • Iceland • remote sensing • Arctic • ArcGIS • mapping

1. Introduction

Using remote sensing data for environmental analysis is motivated by complex relationship between the landscapes and factors affecting their formation. Land cover types visible on the Earth's surface reflect geographic and geologic processes that influenced landscape formation. Specifically, the distribution of the land cover types is controlled by geologic, climate, soil and geomorphological factors that finally affect the vegetation

patterns of the landscapes. The information regarding such correlations and processes can be revealed from the analysis of the satellite images using advanced methods of GIS for image processing.

A variety of factors affect landscapes and control land cover types. For example, negative consequences of climate changes and anthropogenic activities on the landscapes have environmental effects. These may include negative impacts on vegetation (crops, canopy, forests), affected biodiversity [Abdi et al. 2021] or degradation of soils caused by the or intensive farming or grazing [Ali et al. 2016]. As a consequence, declines in crops affects socio-economic development of farming and biodiversity [Fahrig 2003, Mendenhall et al. 2014, Rappaport et al. 2020]. Therefore, balanced, and sustainable land use is a necessary prerequisite for effective farming. In turn, land use changes can effectively be studied using remote sensing data processing and visualization of the vegetation indices, such as NDVI.

The risks of biodiversity losses can also be estimated using remote sensing data derived from the satellite images such as Landsat TM/ETM+. The biodiversity loss and environmental changes are strongly associated with climate, environmental and anthropogenic effects [Wilson et al. 2017, Yan et al. 2021]. The example of the anthropogenic effects affecting vegetation health include overuse of fertilizers and pesticides, while the examples of the hazardous climate events include droughts, floods, temperature fluctuations, intense precipitation, soil dryness. Complex effects from the anthropogenic and natural factors on vegetation lead to the land cover changes visible on Earth surface that can be detected using satellite imagery such as Landsat TM [Xie 2008, Weiss et al. 2020].

Climate changes and negative environmental processes are well reflected in vegetation health. This information can be derived from the satellite images [Colwell 1981, Challinor et al. 2018, Peng et al. 2020]. Based on the fundamental remote sensing principles [Colwell 1981], vegetation health can be numerically estimated and assessed on a pixel-based level as a spectral reflectance of leafs and canopy [Daughtry 2001, Suomalainen et al. 2021]. In this study, the remote sensing data analysis has been performed based on the computed NDVI formula of vegetation indices, following existing examples of studies on vegetation indices [Chen et al. 2010, Yangci et al. 2014, Olson et al. 2019, Zhi et al. 2019]. This approach is based on computing combinations of various spectral bands of the Landsat TM satellite image that can be applied for vegetation mapping aimed at precision farming.

The complexity of the environmental processes can be better studied using robust methods of GIS for processing remote sensing data. Therefore, using spatial analysis by GIS applied for satellite imagery allows to determine contours of the distribution of various land cover types and vegetation areas. Deriving information on vegetation greenness, health, and leaf area index (LAI) is possible using GIS functionality and Landsat TM data. Effective machine learning approach of image processing includes mapping land cover types and calculating Normalized Difference Vegetation Index (NDVI) to map vegetation greenness [Crippen 1990, Lemenkova 2015, 2020a, 2020b, Lassalle et al. 2019, Li et al. 2019, Zhang et al. 2020].

The use of GIS for image processing enables not only to visualize satellite imagery using the RGB colour composites of band combinations, but also to perform classification (e.g., ISOCLUST) and calculate NDVI. From a geographical point of view, landscape diversity in Arctic regions is affected both from the natural reasons (climate, geology, soils) and human-induced aspects (overgrazing, land use). Nevertheless, correct combination of the colour composites enables to highlight specific land cover types such as natural reserves and forests.

The aim of this study is to determine vegetation on the multispectral Landsat TM image by raster calculation using ArcGIS. The practical goal was to compute NDVI, map land cover types and visualize colour composites using band combinations. The combination of the Landsat bands can be effectively used for mapping landscapes, because vegetation has spectral reflectance that varies from other land cover types in various combinations of spectrum [Mccloy 2006]. Landsat TM is a multispectral image containing various bands, such as red, green, blue, or near-infrared electromagnetic spectrum, which explains its suitability for vegetation mapping.

The study area is located in northern Iceland (17.00°W–23.00°W, 64.30°N–67.00°N), Fig. 1. The vegetation growth in Iceland is strongly affected by a variety of factors which is reflected in a complex pattern of various land cover types. Harsh climate conditions and specific geologic settings, such as volcanism, result in the erosion of soils. The anthropogenic factors affecting land cover types include overgrazing of cattle. Moreover, ecosystems in Iceland consist of the complex composition of species including two types of species: Atlantic European and sub-Arctic. Monitoring such complex and vulnerable Arctic environment takes advantages from the advanced geoinformation methods and remote sensing data.

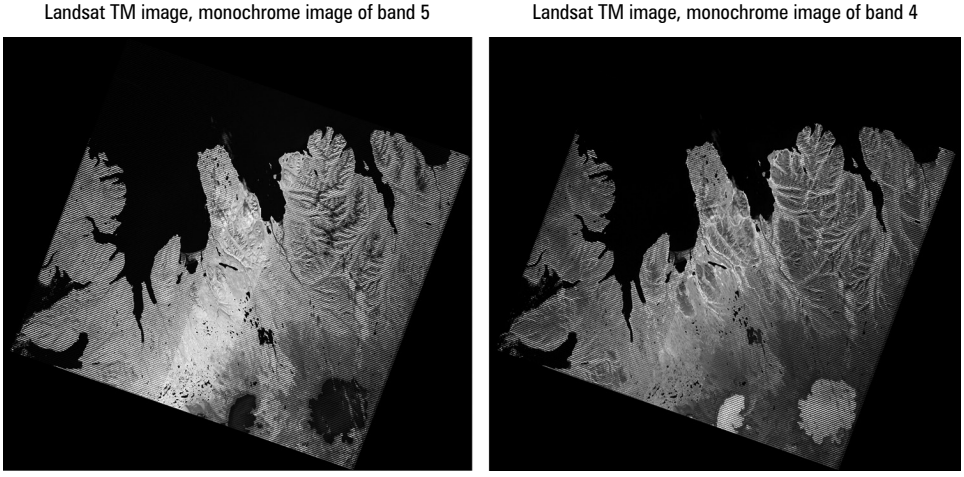

Source: Author's own study

Fig. 1. Bands 4 (R) and 5 (NIR) used for the NDVI calculations

2. Materials and methods

2.1. Colour composites

The Landsat scene taken on 2001/09/08 was downloaded from the GloVis repository. The coordinates are set up in a UTM North coordinate system, WGS_1984_UTM_Zone_27N, for Iceland. At the first step of processing, the GeoTIFF tiles of the Landsat TM image were navigated in the GloVis repository, downloaded and imported to the ArcMap menu. Afterwards, the bands of the Landsat TM image were selected for combination of the colour composite and displayed in the ArcGIS menu. Creating colour Composites has been done using the Arc Toolbox menu of the ArcGIS. The image was opened as RGB display in a UTM coordinate system using various bands combinations. The cartographic elements were added via the property's menu of the map layout: legend, scale bar, north arrow, grid as graticule. The map was exported and saved in the conventional graphical format (JPG).

The colour composites were generated using combinations of various bands. Trial band combinations have been performed for detecting vegetation to find the best view of the landscape patches. The comparison of various vegetated and non-vegetated areas with the corresponding colours in different band combination assured the correct interpretation of the image. For example, standard 'false colour' composite 4-3-2 (Fig. 2, left) shows vegetation coloured in shades of reds, at that the shades differ as such: coniferous plants appear darker red than broadleaf (birch, rowan) which appears crimson. The interpretation of other band combinations is explained in the relevant section (Results) of this manuscript.

2.2. NDVI calculation and visualization

The NDVI is a combination of visible red (R) and a near infrared (NIR) bands of the electromagnetic spectrum of Landsat TM image. The NDVI ranges in value from –1.0 to 1.0. It is used to measure the vigour of vegetation on the Earth. The equation used for the NDVI calculation is NDVI = (NIR – R)/(NIR + R), where NIR and R are the values of pixels in these bands, respectively. Originally displayed as monochrome images (Fig. 1), the combined bands give colour composite.

The NDVI is based on the following approach to quantify healthy vegetation. The NIR band is used because vegetation has high spectral reflectance in this region, while plants are strongly absorbing red. Using such property of vegetation, the difference between NIR and R enables to highlight and contour areas of the green canopy on the satellite image. As a result, NDVI is useful to measure greenness and health of vegetation for agricultural, forestry and ecological studies. For instance, calculating NDVI by band combination can be applied for analysis of greenness and health of leaves in individual trees (dryness, diseases caused by insects and beetles, fungi, pests, mould) and also detecting weeds among the crops. Therefore, the NDVI is useful for comparative analysis of vegetation health on the remote sensing data. Visualizing of NDVI may also include a time series showing changes and trends in environmental

parameters. Specifically in this study, we aim to perform image analysis for mapping vegetation using based on the Landsat TM multi-spectral image processing for visualization of the leaf greenness. The process of information retrieval from the raw Landsat TM image includes image processing and classification by the algorithms in ArcGIS.

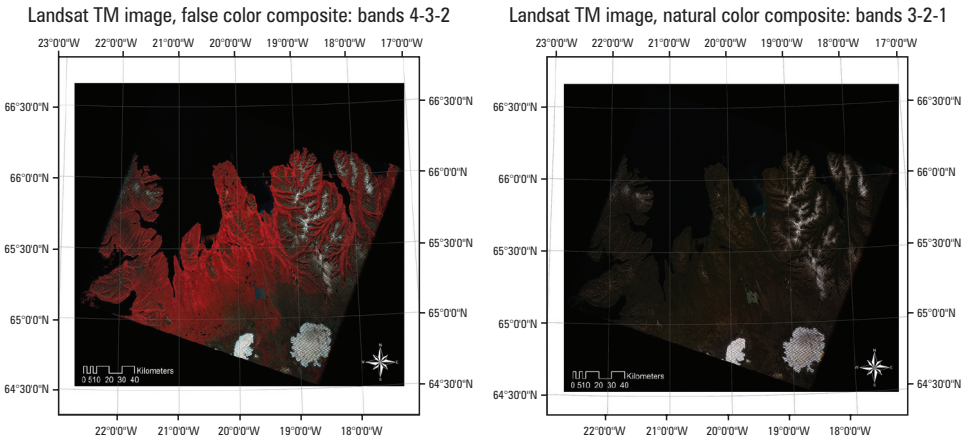

Source: Author's own study

Fig. 2. Colour 4-3-2 composites (red-green-blue) and 3-2-1 (green-blue-aerosol)

2.3. ISOCLUST classification

The ISOCLUST classification of satellite image is based on the principle of data partition, sorting, and grouping to the classes (clusters) using similarities in their values. The idea of data clustering has been applied in many studies demonstrating data sorting [Lemenkova 2013, 2020c]. The mathematical algorithms of data grouping and clustering are described in theoretical studies [Davies and Bouldin 1979] and practical applications [Lemenkova 2019a, Xu and Wunsch 2005, Rubin 1967]. The ISOCLUST algorithm was used in ArcGIS for clustering pixels on the Landsat TM image. This method consists in assignments of pixels into a number of classes.

The ISOCLUST classification method consists in the iterative optimization clustering which separates the cells on the raster image into the specified number of distinct groups in the space of the input bands [Ball and Hall 1965, Richards 1986]. In this study we selected 8 classes (Fig. 10). The ISOCLUST tool was selected because it is the most useful approach for the unsupervised classification of the satellite images since its development. In this study, nine clusters were selected as representative for the landscapes and requiring the optimal number of iterations. Each cluster on the output image (Fig. 10) contained enough cells to accurately represent the cluster. The DNs of pixels (spectral reflectance) were assessed to form nine groups of pixels.

3. Results

Figure 2 shows the 4-3-2 band combination (red-green-blue), which is useful for vegetation and agricultural monitoring and distinguishing it from soils and growing crop.

In this band combination the broadleaf healthy vegetation has a deeper red hue while lighter colours point at the grasslands or sparsely vegetated areas. Soils varying from dark to light browns. The ice-covered areas, glaciers, and snow in the mountains near the fjords are white-coloured. The populated urban areas of Sauðárkrókur in the Skagafjörður fjord and Akureyri in the Eyjafjörður fjord are shown in steel-grey to blue. This 4-3-2 band combination resembles the traditional colour infrared aerial photography (Fig. 2).

The 'natural colour' band combination 3-2-1 (green-blue-coastal aerosol) is shown in Figure 2, right. This combination is based on the visible bands. Therefore, objects and land cover types are resembling their appearance to the eye's: vegetation is dark green and selected species are hard to distinguish, while agricultural fields have very light yellowish hues, dry vegetation is brown, urban settlements are steel grey, clouds and ice are white and hard to separate. Mostly used for urban studies, this band combination has a lesser interest for agricultural studies, because cleared and sparsely vegetated areas are also hard to detect. Another drawback of the 'natural colour' combination is that it does not distinguish shallow water from soil and therefore both look in dark brown colours.

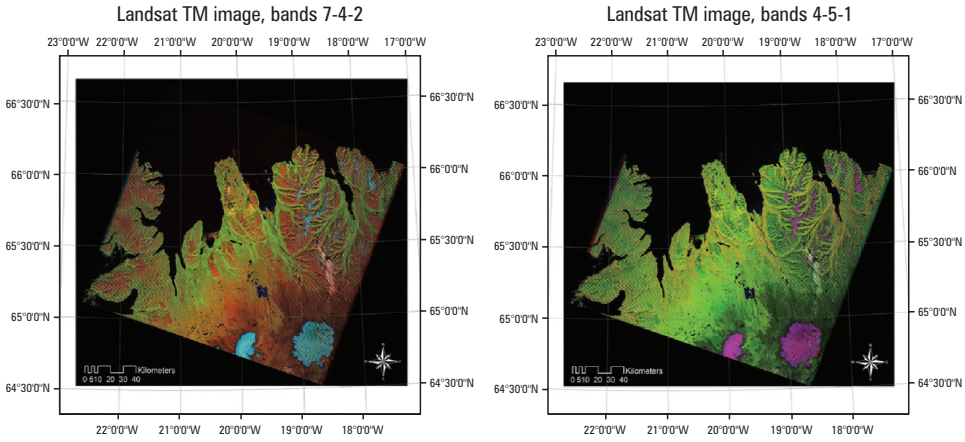

Source: Author's own study

Fig. 3. Colour composites 7-4-2 (SWIR-red-blue) and 4-5-1 (red-NIR-aerosol)

Figure 3 shows the 7-4-2 bands combination shows a mix of mid-infrared-red-blue channels of the Landsat TM (Fig. 3, left). This combination provides a natural-like appearance, but comparing to the 3-2-1 bands (Figure 2, right), the healthy vegetation appears as an acid bright green. Grasslands and agricultural areas near the Varmahlíð

appear green. Hues of orange colours and brownish represent sparsely vegetated areas around the Akrahreppur municipality. Dry vegetation is coloured orange and ice-covered areas are blue (clearly visible Hofsjökull and Langjökull glaciers, the third and second largest glaciers in Iceland, respectively), water areas (Blöndulón lake) are dark blue to black). Sands and soils are highlighted in a variety of colours.

Since the areas of vegetation and plants are clearly distinguishable, this band combination is useful for agricultural studies. In contrast to the coniferous (olive-green) and broadleaf (bright green), grasslands appear as lighter green. The 7-4-2 combination (Fig. 3, left) in general resembles the 5-4-3 (Fig. 5, left) in that healthy vegetation is coloured bright green. However, the 5-4-3 bands are better fixed for the agricultural studies due to the presence of near-infrared channel. The 4-5-1 combination of the red-NIR-aerosol Landsat bands (Fig. 3, right) is more useful for fire monitoring burnt forest areas, because band 4 (NIR) emphasizes biomass content, while band 5 (Short-wave Infrared) well discriminates moisture content of soil and vegetation. Besides, it shows the Hofsjökull and Langjökull glaciers and smaller ice-covered areas in the mountains as bright magenta, so it can be used for glacial studies.

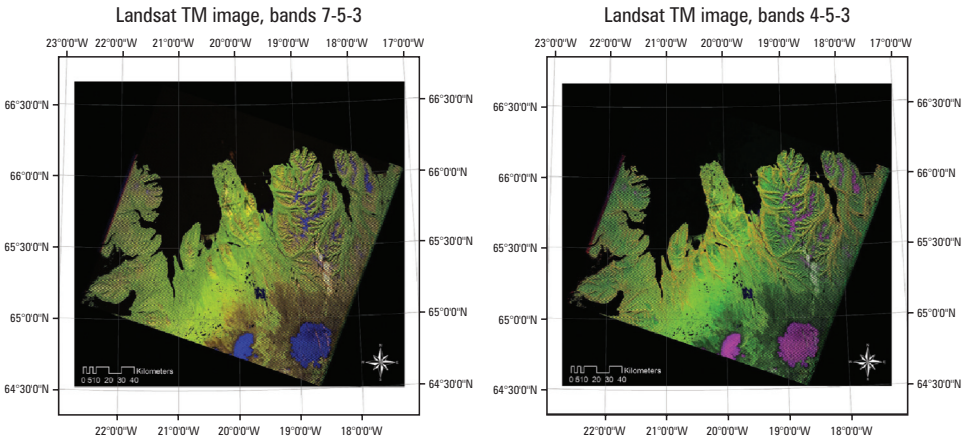

Source: Author's own study

Fig. 4. Colour composites 7-5-3 (SWIR2-NIR-green) and 4-5-3 (red-NIR-green)

Figure 4 (left) shows the 7-5-3 combination which provides a natural-like view of the landscapes with the removal of the atmospheric effects: growing vegetation is coloured in shades of green depending on the type (coniferous, broadleaf) and healthy state. The grasslands near the Möðruvellir surroundings appear yellow greenish. The urban features in the municipalities of Blönduós and Þingeyrar farm adjacent to the sandy coasts are coloured gray. The mountainous areas with base soils, sands and minerals appear in a variety of brown colours contrasting with bright blue colour of the Hofsjökull and Langjökull glaciers. The almost complete absorption of SWIR-2 (short-

wave infrared bands) in water area of the Norwegian Sea coloured black provides well distinguishable coastlines. Water bodies are very dark blue (Blöndulón lake) or black along the Norwegian Sea coasts, which is clear and contrasting compared with the 3-2-1 natural colour band combination in which water is coloured grey and difficult to distinguish.

Figure 4 (right) shows band combination 4-5-3, which presents red-NIR-green bands of the Landsat TM scene. Here, the clearly distinguishable areas demonstrated ice-covered regions and two glaciers, the Hofsjökull and the Langjökull. This combination clearly defines land-water boundaries and therefore, highlights details not apparent in the visible bands. Thus, lakes and rivers (Svínavatn, Hóp and local rivers) are detected with greater precision due to the infrared bands. With the 4-5-3 band combination, vegetation type and health show as variations of hues (brown, green and orange) and tone along the river valleys in the mountainous region in the Skagafjörður and Eyjafjörður fjords. Moreover, the 4-5-3 combination better detects soil and vegetation conditions due to the moisture differences between the soil and vegetation: darker colours of soil are typical for the wetter areas along the coasts of shelf area in the Norwegian Sea, due to the infrared absorption of water.

Figure 5 shows that healthy vegetation appears in shades of orange and yellowish with hues for various vegetation types (e.g., sparse grasslands are coloured grey), soils are shown in greens. However, agricultural areas and natural vegetation types are mixed and not well distinguishable on an image. Clear, deep water in the ocean areas (coasts of the Norwegian Sea) is black to dark blue in the combination 5-4-3 (SWRI-NIR-red). Shallow inland waters appear as shades of light blue (e.g., the Blöndulón lake), and ice-covered areas as bright magenta. For vegetation studies, the addition of the infrared band in this combination enables to detect various stages of plant growth and canopy.

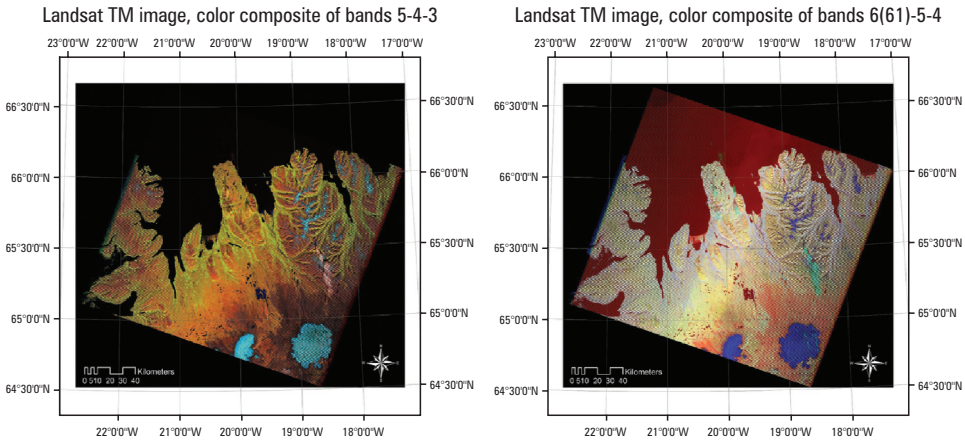

Source: Author's own study

Fig. 5. Colour composites 5-4-3 (NIR-red-green) and 6-5-4 (SWIR1-NIR-red)

Figure 5 (left) shows band combination of 5-4-3 (NIR, red, green) (includes the infrared bands which is advantageous for vegetation: here, the healthy vegetation appears brick red and bright orange depending on the plant type. Similar to the combination 7-4-2 (SWIR-red-blue), in Figure 3 (left) this image provides information on vegetation distribution, contours of river valleys and geomorphological patterns of landforms through the colour contrast. Healthy vegetation is bright green, as can be seen in the surroundings of Blönduós village. The urban populated areas of Hvammstangi appears brownish and bare soils are mauve. The 5-4-3 band combination is the most effective for agricultural mapping and vegetation studies due to the effective distinguishability of colour showing land cover types and vegetation health in contrasting colours. Figure 5 (right) shows band combination of 6-5-4 (SWIR1-NIR-red), which is useful both for vegetation analysis and general land cover types mapping: the glacier areas appear bright blue colours, clouds are cyan and can be well distinguished, healthy vegetation appears in light grey colours, water in maroon.

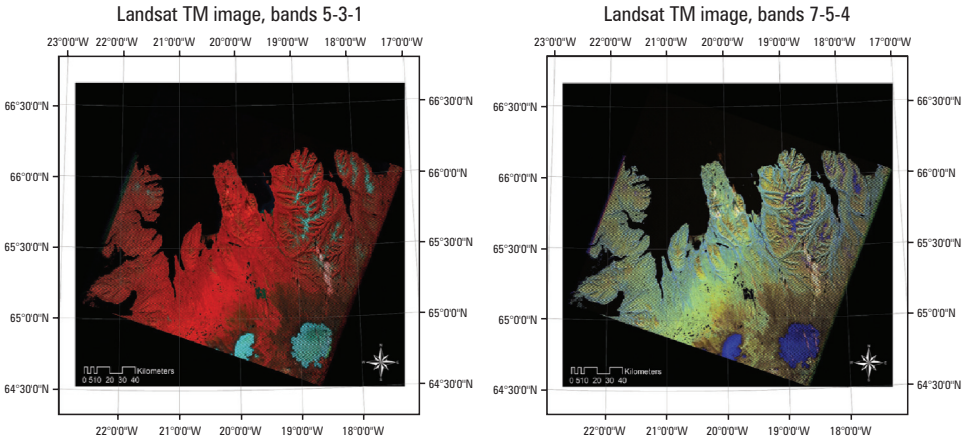

Source: Author's own study

Fig. 6. Colour composites 5-3-1 (NIR-green-aerosol) and 7-5-4 (MIR-NIR-red)

Figure 6 (left) shows the band combination 5-3-1 (NIR-green-aerosol) which resembles the false colour composites shown in Figure 2 showing the 4-3-2 composite (red-green-blue). However, here the vegetation appears more bright scarlet colour and is hardly to be distinguished from other land cover types. The 5-3-1 combination better displays the topographic patterns and geomorphological textures (elevations, hills, and detailing relief in the mountainous areas). The combination of bands 7-5-4 (SWIR2-NIR-red). The 7-5-4 combination (Fig. 6, right) presents SWIR2, NIR and red bands providing the best atmospheric penetration. Here the coast lines of the Norwegian Sea are well defined with contrasting black colours of waters. This combination highlights soil properties including texture and moisture. Shallow lakes are very dark blue while

ice-covered areas and glaciers are coloured as bright blue (Hofsjökull, Langjökull and minor glaciers in the mountains).

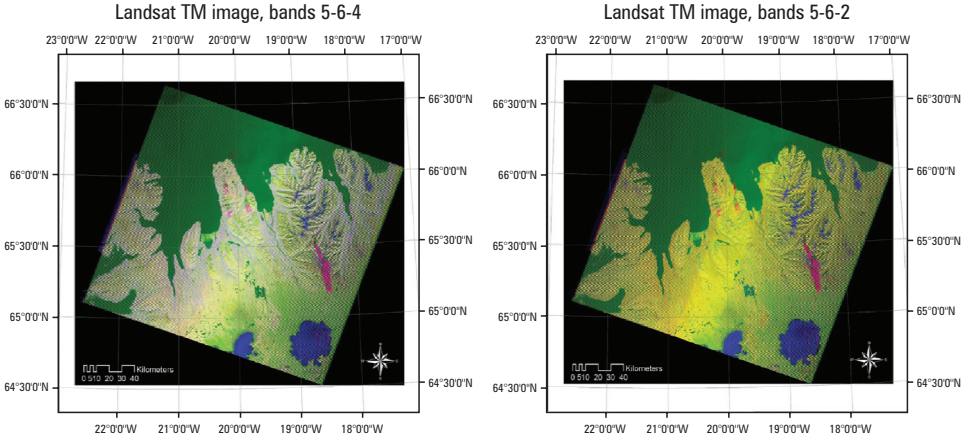

Source: Author's own study

Fig. 7. Colour composites 5-3-1 (NIR-green-aerosol) and 5-6-2 (MIR-NIR-red)

Figure 7 (left) shows land-water distinguishability is best represented on the band combination 5-3-1 showing NIR, SWRI1 and red bands. The water areas appear in bright green colours, clouds are bright pink, glaciers are coloured bright blue. The vegetation, however, appears as less distinguishable being coloured as dim grey colours and can be mixed with the soil (coloured as light yellowish green). Band combination of 5-6-2 in Figure 7 (right) is composed by the NIR, SWIR1 and blue bands of the Landsat TM image. It depicts healthy vegetation as olive green in contrast with the dry grasslands and bare soils. As in combination of 5-6-4, clouds appear pink coloured, ice glaciers are bright blue, and water is green. In contrast with the previous image (Fig. 7, left), bare soils are coloured brighter and contrasting yellowish green, against light green, and therefore, are better distinguished.

Figure 8 (left) shows colour composites 7-3-1 (SWIR-2-green-aerosol) which looks similar to the band combination of composites 5-3-1 (NIR-green-aerosol) in Figure 6 (left), which is caused by the similarities of band mix including both visible bands and an infra-red band. Although the vegetation here appears bright red to crimson red, it is hardly distinguishable from the surrounding land cover types and can be easily mixed with resulting misclassified pixels. Such a combination can still be used to display differences in the rock types.

Figure 8 (right) shows the combination of 6-5-2: SWIR1, NIR and blue bands of the Landsat TM. Due to the presence of infra-red bands, it well depicts agricultural fields and various vegetation types. The grasslands in the surroundings of the near the Árneshreppur and Hólmavík municipalities are highlighted as light yellowish green.

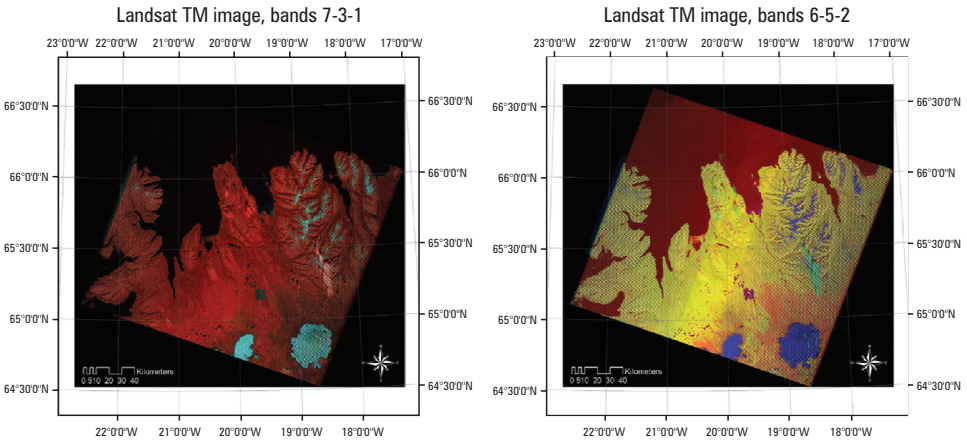

Source: Author's own study

Fig. 8. Colour composites 7-3-1 (SWIR-2-green-aerosol) and 6-5-2 (SWIR1-NIR-blue)

Figure 9 (left) shows band combination 7-6-4, that are false colour composite. This band combination is better suited for urban mapping rather than agricultural studies, because the vegetation here is coloured green in various types so can be easily mixed with grassland and coastal flatlands. The band combination 5-4-2 (Fig. 9, right) highlights the water and soil together in a Landsat TM image as light yellowish hues.

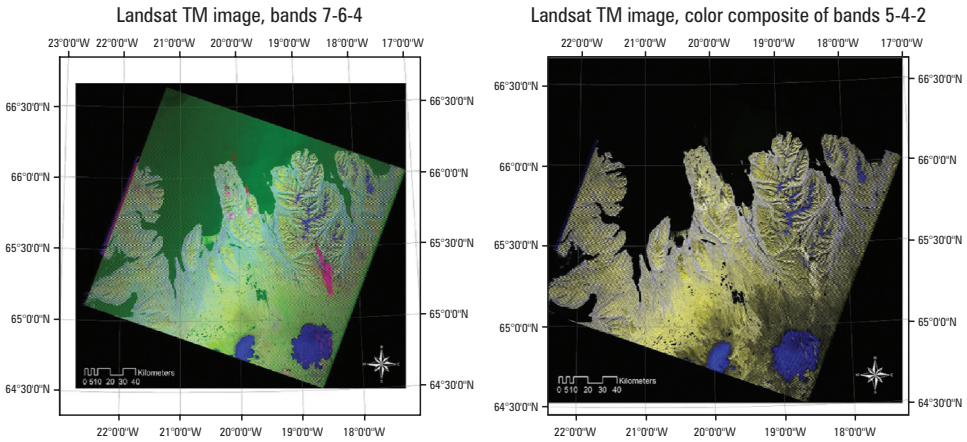

Source: Author's own study

Fig. 9. Colour composites 7-6-4 (SWIR-2-SWIR-1-red) and 5-4-2 (NIR-red-blue)

Different colour composites of Landsat TM image enable to reveal various land cover types and have many applications in existing studies. Examples include discriminating natural vegetation from agricultural lands, detecting, and contouring cities, monitoring vegetation or pasture degradation [Suriga et al. 2012, Nagendra et al. 2013]. Other cases include geologic mapping [Tripathi and Govil 2019], estimating biomass of vegetation [Li and Liu 2004] or climate and meteorological studies [Lv et al. 2017].

Besides, trial testing of various colour composites enables to find or better detect various phenomena which makes them useful in various practical applications. To mention some of them: indirect parameters of soil types that can be assessed using colour composites of the images, relief parameters reflected in vegetation types (indirectly affected by slope steepness, terrain ruggedness, slope aspect related to the solar intensity, flow direction and intensity that induces soil erosion), as well as hydrologic parameters (river drainage network: density and curvature), and soil types.

3.1. Mapping land cover types by ISOCLUST

The results of the land cove mapping using the ISOCLUST approach (Fig. 10) show nine well separated classes. The algorithm separated the classes which were named by the user in post-processing stage including the following types: vegetation areas (magenta, class 6), water bodies including deep ocean areas and inland lakes (blue, class 2), agricultural areas and crop fields (beige, class 1), coniferous forests (dark green, class 4), broadleaf forests such as rowan, birch (light green, class 3), ice-covered areas and glaciers (yellow, class Nr. 8), bare soils (brown, class 5), rock minerals and mountain areas (purple, class 7).

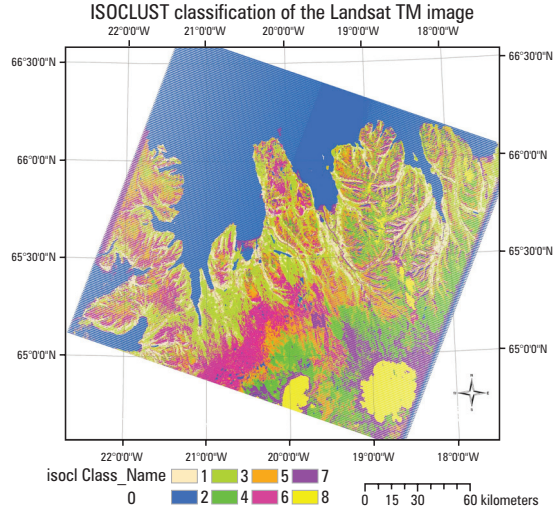

Source: Author's own study

Fig. 10. Classified Landsat TM image using ISOCLUST approach, ArcGIS

3.2. Estimating NDVI

This study used existing methods of computation of NDVI using review on the vegetation indices [Somvanshi and Kumari 2020]. The NDVI is a robust indicator used to analyse the Landsat TM scene and assess whether the land cover types observed in northern Iceland contains healthy green vegetation. Moreover, among the advantages of the NDVI in environmental studies that should be mentioned is the emphasized colour of the vegetation canopy rather than its brightness. This enables to avoid this effect from local geomorphology that affects the intensity of the visualized image through shadows from the elevated landforms (hills and valleys). The high and low vegetation were classified using the ArcGIS NDVI raster calculation. Pixels with high NDVI values indicate high vegetation or chlorophyll (0.06 to 0.41, coloured beige in Figure 11). In contrast, low NDVI values mean less vegetation.

Upon creating the NDVI, a histogram statistic was visualized to demonstrate frequency of pixels' distribution over the study area (Fig. 11). The image is coloured with a colour palette that ranges from cold colours in strong negative values (magenta, purple, blue and cyan) to green (aquamarine and lane green) for slightly negative values and the last group is for positive values (orange and brown). No values are represented by white as a 'zero-class' group. The lowest negative values (–0.89 to –0.68) show the ice-covered areas (bright magenta colours in Figure 11).

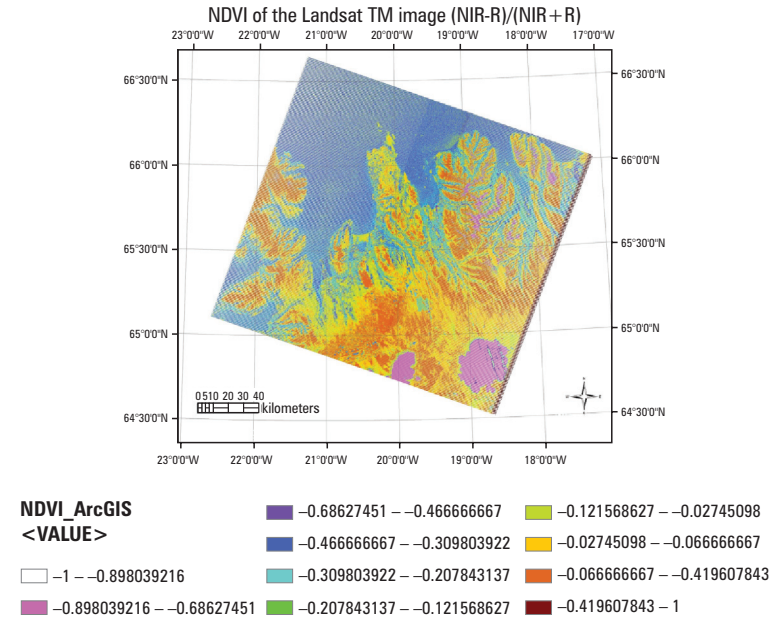

Source: Author's own study

Fig. 11. Computed NDVI map for the Landsat TM image. ArcGIS

Two colours of blue represent two types of water: the deep ocean areas (dark blue with –0.68 to –0.46) and shallow coastal areas (–0.46 to –0.30, blue areas in Figure 11). The inland lakes are shown as cyan colours (group of –0.30 to –0.20). The urban areas are shown in a group –0.20 to –0.12. The highest values (0.4 to 1, displayed as dark brown) indicate forests with dense green leaves. The low values of NDVI around the value of zero (–0.11 to –0.02, lane green in Figure 11) corresponding to the barren areas of rock minerals in the mountains and sand. Slightly negative to very low positive values (–0.02 to 0.06, beige) show bare soils. Low positive values (0.06 to 0.41) show shrub and grassland.

NDVI calculation enables to detect health/disease of leaves and vegetation greenness of crops. Therefore, computing NDVI using RS data (Landsat TM) in an automated regime has a practical application for environmental analysis. Using NDVI is a widely used practice in controlling and visualizing disease in leaves. Besides, mapping NDVI for smart monitoring of vegetation health by satellite images such as Landsat TM/ETM+ may contribute to the precision agriculture solutions (by comparing the period of the image intake, exact location of the study area and overlay, healthy or affected plants) and monitoring using vegetation indices, such as NDVI. There are various vegetation indices, apart from the NDVI. However, the NDVI is by far the most widely used and accepted in environmental monitoring of vegetation due to its effectiveness and robustness.

4. Discussion

Besides the NDVI, there are other vegetation indices that can be computed using the multispectral images: SAVI, PVI, EVI, BRVI, SRVI and many other [Qi et al. 1994, Rondeaux et al. 1996, Walter-Shea et al. 1997, Mroz and Sobieraj 2004, Hüttich et al. 2009, Zhang et al. 2016]. Over 20 vegetation indices based on the VNIR spectrum have been reviewed and compared in the existing study [Silleos et al. 2006]. The indices are generated by adding and removing bands in various combinations, showing their different proportions in imagery.

The data for land cover mapping may include not only Landsat TM but also other satellite sensors that have the necessary bands with NIR and red: MODIS, SPOT, or AVHRR [Cross et al. 1991, Kaufman and Tanre 1992, Kerdiles and Grondona 1995, Khan et al. 2010]. Examples of the satellite images include LiDAR, RaDAR, and Stereo Data [Pabi et al. 2020]. However, other vegetation indices might be tied to the specific bands or require a pre-computed NDVI. In view of this, computing the NDVI presents the most standardized approach to highly effective in the environmental and agricultural monitoring. Therefore, it is most common index used in remote sensing [Taufik et al. 2016, Pradeep Kumar et al. 2020, Westinga et al. 2020]. Based on the principle that healthy green vegetation (chlorophyll) reflects more NIR and green light against other wavelengths, and absorbs more red and blue light, the usage of NDVI makes it effective algorithm in vegetation and agricultural studies.

As demonstrated in this study, data derived from the processed Landsat TM image highlight specific phenomenon of the spectral reflectance of plants. For instance, an

NDVI shows healthy vegetation in a bright colour while diseased vegetation has lower values and desert areas appear darker. More detailed studies based on the advanced methods of neural network and deep learning enables to apply a combination between colour spaces and vegetation indices for detection of diseased plants [Kerkech et al. 2018], phenological type analysis [Bauer et al. 2019], vegetation stress assessment [Butte et al. 2021], identification of the trees [Onishi and Ise 2021], land use classification [Campos-Taberner et al. 2020] or cultivation and management of horticulture crops [Yang and Xu 2021].

The sixteen combinations of colour composites were visualized and the behavior of the spectral reflectance's of various land cover types was analysed to assess usability in vegetation studies. Although NDVI ranges from –1 to +1, a distinct boundary for the land cover types is not clear in the NDVI modelling. Therefore, the additional ISOCLUST classification was done to detail the land cover types. The results of this study include the mosaic of landscape patterns made by trial combinations of colour composites (Fig. 1 to 9), mapped land cover types by ISOCLUST classification (Fig. 10) and computed NDVI with nine classes (Fig. 11).

A recommendation for future studies includes the expansion of methods and data towards data-driven research. Among the most important methods we recommend time-series analysis using several Landsat TM/ETM+ images covering the same area which would enable to perform a retrospective analysis of vegetation based on modern state and historical data. Another advice consists in the comparative spatial analysis that can be performed using various layers such as topographic maps, crop distribution and environmental/weather conditions for perspective mapping of prognosis and vegetation analysis in various regions of Iceland or similar regions in the Arctic.

Finally, based on the data availability, the topographic mapping can be expanded using LiDAR/DEM for detecting hydrological aquifers in the study area. This would be actual, for instance, to get a closer look at the selected areas of fjords and rivers of Iceland. The extent of aquifers shows water storage capacity, runoff direction and drainage that can be used as an information for spatial analysis and hydrological modelling aimed at environmental risk assessment.

5. Conclusion

This study focused on a quantitative and qualitative analysis of vegetation coverage in Iceland by the ArcGIS to reveal its application for the remote sensing studies. The GIS is often used for thematic vector-based mapping in socio-economic studies [Czajka and Szczepaniak-Koltun 2017, Klaučo et al. 2017], environmental monitoring [Suetova et al. 2005a, 2005b, Klaučo et al. 2013, Babiy et al. 2017, Lemenkova 2020d, 2021a, 2021b], or web mapping [Jianhua and Zhenwen 2012, Hao et al. 2014, Yang et al. 2017]. In this study ArcGIS was used for image processing, NDVI calculations and an unsupervised classification. Besides the studies on soil and vegetation in Iceland, a comparative analysis on colour composites of the Landsat TM, NDVI and ISOCLUST clustering has been presented in this study. The paper demonstrated the use of the ArcGIS for vegeta-

tion mapping with use of NDVI, ISOCLUST and combinations of colour composites.

The results of the NDVI calculations, a standardized vegetation index, shown the presence and condition of vegetation, that is, a relative biomass, in the area of northern Iceland. The NDVI was applied based on the contrast of characteristics of two channels from a multispectral Landsat TM raster dataset: the absorption of chlorophyll by the pigment in R channel and, in contrast, high reflectivity of plants in NIR. Using such a contrast of spectral behaviour, the map of the vegetation distribution was presented. The ISOCLUST unsupervised classification performed by ArcGIS enabled to identify nine clusters of the land cover types in northern region of Iceland. Additionally, the NDVI simulation was utilized for analysis of different vegetation types and health (greenness and leaf area index). colour composites of bands show suitability of this method to highlight land cover types. The land cover types address environmental processes in northern Iceland and represent cartographic approaches of the ArcGIS-based research in agricultural mapping.

The presented results are based on using the ArcGIS software and a Landsat TM image, which should be noted if comparing with other GIS tools and data. Extending this research to other imagery datasets, such as SPOT, MODIS, Sentinel and AVHRR would be ideally to compare as a time series for the assessment of land cover changes. Progress in GIS and machine learning algorithms in cartography propose a multidisciplinary use of mapping techniques [Schenke and Lemenkova 2008, Teganya and Romero 2020, Lemenkova 2019b, 2019c]. These can be used in the environmental studies on vegetation to receive knowledge on local landscape features and species. Present research contributed to the use of algorithms of the machine-based image classification for environmental studies using ArcGIS.

Acknowledgements

The author would like to thank the two anonymous reviewers for their careful reading, helpful comments and suggestions which improved the earlier version of this manuscript.

References

Abdi A.M., Carrié R., Sidemo-Holm W., Cai Z., Boke-Olén N., Smith H.G., Eklundh L., Ekroos J. 2021. Biodiversity decline with increasing crop productivity in agricultural fields revealed by satellite remote sensing. Ecological Indicators, 130, 108098. https://doi.org/10.1016/j.ecolind.2021.108098

Ali I., Cawkwell F., Dwyer E., Barrett B., Green S. 2016. Satellite remote sensing of grasslands: from observation to management. Journal of Plant Ecology, 9(6), 649–671. https://doi.org/10.1093/jpe/rtw005

Babiy L., Hrytskiv N., Laykun L. 2017. Thematic mapping of avalanche-threatened areas. Geomatics, Landmanagement and Landscape, 4, 15–26. https://doi.org/10.15576/GLL/2017.4.15

Ball G.H., Hall D.J. 1965. A Novel Method of Data Analysis and Pattern Classification. Stanford Research Institute, Menlo Park, California.

Bauer A., Bostrom A.G., Ball J., Applegate C., Cheng T., Laycock S., Rojas S.M., Kirwan J., Zhou J. 2019. Combining computer vision and deep learning to enable ultra-scale aerial

phenotyping and precision agriculture: A case study of lettuce production. Horticulture Research 6, 70. https://doi.org/10.1038/s41438-019-0151-5

Butte S., Vakanski A., Duellman K., Wang H., Mirkouei A. 2021. Potato Crop Stress Identification in Aerial Images using Deep Learning-based Object Detection. Agronomy Journal, 00,1–12. https://doi.org/10.1002/agj2.20841

Campos-Taberner M., García-Haro F.J., Martínez B., Izquierdo-Verdiguier E., Atzberger C., Camps-Valls G., Gilabert M.A. 2020. Understanding deep learning in land use classification based on Sentinel-2 time series. Scientific Reports, 10, 17188. https://doi.org/10.1038/s41598-020-74215-5

Challinor A.J., Müller C., Asseng S., Deva C., Nicklin K.J., Wallach D., Vanuytrecht E., Whitfield S., Ramirez-Villegas J., Koehler A.-K. 2018. Improving the use of crop models for risk assessment and climate change adaptation. Agricultural Systems, 159, 296–306. https://doi.org/10.1016/j.agsy.2017.07.010

Chen X., Zhang X., Zhang L., Liu H. 2010. NDVI data continuity between Beijing-1, TM, and SPOT. 2010 Second IITA International Conference on Geoscience and Remote Sensing, 2010, 202–205. https://doi.org/10.1109/IITA-GRS.2010.5602974

Czajka A., Szczepaniak-Koltun Z. 2017. Analysis of transaction price of undeveloped real estate of Kołobrzeg with the use of GIS technology. Geomatics, Landmanagement and Landscape, 4, 27–37. https://doi.org/10.15576/GLL/2017.4.27

Colwell R. 1981. Remote Sensing and Spatial Information. Nature, 293, 364. https://doi.org/10.1038/293364a0

Crippen R.E. 1990. Calculating the vegetation index faster. Remote Sensing of Environment, 34, 71–73. https://doi.org/10.1016/0034-4257(90)90085-Z

Cross A.M., Settle J.J., Drake N.A., Pävinen R.T.M. 1991. Subpixel measurement of tropical forest cover using AVHRR data. International Journal of Remote Sensing, 12, 1119–1129. https://doi.org/10.1080/01431169108929715

Davies D.L., Bouldin D.W. 1979. A cluster separation measure. IEEE Transactions on Pattern Analysis and Machine Intelligence PAMI, 1(2), 224–227. https://doi.org/10.1109/TPAMI.1979.4766909

Daughtry C.S.T. 2001. Discriminating crop residues from soil by shortwave infrared reflectance. Agronomy Journal, 93, 125–131. https://doi.org/10.2134/agronj2001.931125x

Fahrig L. 2003. Effects of habitat fragmentation on biodiversity. Annual Review of Ecology, Evolution, and Systematics, 34 (1), 487–515. https://doi.org/10.1146/annurev.ecolsys.34.011802.132419

Hao J., Pan M., Wang D., Zhao L., Zhao D. 2014. A new web chart service and applications system based on arcgis. Proceedings of the 33rd Chinese Control Conference, 3411–3414. https://doi.org/10.1109/ChiCC.2014.6895504

Hüttich C., Gessner U., Herold M., Strohbach B.J., Schmidt M., Keil M., Dech S. 2009. On the suitability of MODIS time series metrics to map vegetation types in dry savanna ecosystems: a case study in the Kalahari of NE Namibia. Remote Sensing, 1(4), 620–643.

Jianhua W., Zhenwen P. 2012. Water Environment Monitoring Information System Based on ASP.NET and ArcGIS Server. 2012 Third World Congress on Software Engineering, 211–214. https://doi.org/10.1109/WCSE.2012.51

Kaufman Y.J., Tanre D. 1992. Atmospherically resistant vegetation index (ARVI) for EOS-MODIS. IEEE Transactions on Geoscience and Remote Sensing, 92, 261–270. https://doi.org/10.1109/36.134076

Kerdiles H., Grondona M.O. 1995. NOAA-AVHRR NDVI decomposition and sub-pixel classification using linear mixing in the Argentinean Pampa. International Journal of Remote Sensing, 16, 1303–1325. https://doi.org/10.1080/01431169508954478

Kerkech M., Hafiane A., Canals R. 2018. Deep leaning approach with colourimetric spaces and vegetation indices for vine diseases detection in UAV images. Computers and Electronics in Agriculture, 155, 237–243. https://doi.org/10.1016/j.compag.2018.10.006

Khan M.R., de Bie C.A.J.M., van Keulen H., Smaling E.M.A., Real R. 2010. Disaggregating and mapping crop statistics using hypertemporal remote sensing. International Journal of Applied Earth Observation and Geoinformation, 12, 36–46. https://doi.org/10.1016/j.jag.2009.09.010

Klaučo M., Gregorová B., Stankov U., Marković V., Lemenkova P. 2013. Determination of ecological significance based on geostatistical assessment: a case study from the Slovak Natura 2000 protected area. Open Geosciences, 5(1), 28–42. https://doi.org/10.2478/s13533-012-0120-0

Klaučo M., Gregorová B., Koleda P., Stankov U., Marković V., Lemenkova P. 2017. Land planning as a support for sustainable development based on tourism: A case study of Slovak Rural Region. Environmental Engineering and Management Journal, 2(1), 449–458. https://doi.org/10.30638/eemj.2017.045

Lassalle G., Credoz A., Hédacq R., Bertoni G., Dubucq D., Fabre S., Elger A. 2019. Estimating persistent oil contamination in tropical region using vegetation indices and random forest regression. Ecotoxicology and Environmental Safety, 184, 109654. https://doi.org/10.1016/j.ecoenv.2019.109654

Lemenkova P. 2013. Monitoring Changes in Agricultural Landscapes of Central Europe, Hungary: Application of ILWIS GIS for Image Processing. Geoinformatics: Theoretical and Applied Aspects. Ukraine, Kyiv, 13–16 May, 2013. https://doi.org/10.3997/2214-4609.20142479

Lemenkova P. 2015. Analysis of Landsat NDVI Time Series for Detecting Degradation of Vegetation. Geoecology and Sustainable Use of Mineral Resources. From Science to Practice. Belgorod, Russia, 11–13. https://doi.org/10.6084/m9.figshare.7211795

Lemenkova P. 2019a. K-means Clustering in R Libraries {cluster} and {factoextra} for Grouping Oceanographic Data. International Journal of Informatics and Applied Mathematics, 2(1), 1–26. https://doi.org/10.6084/m9.figshare.9891203

Lemenkova P. 2019b. Statistical Analysis of the Mariana Trench Geomorphology Using R Programming Language. Geodesy and Cartography, 45(2), 57–84. https://doi.org/10.3846/gac.2019.3785

Lemenkova P. 2019c. AWK and GNU Octave Programming Languages Integrated with Generic Mapping Tools for Geomorphological Analysis. GeoScience Engineering, 65(4), 1–22. https://doi.org/10.35180/gse-2019-0020

Lemenkova P. 2020a. SAGA GIS for information extraction on presence and conditions of vegetation of northern coast of Iceland based on the Landsat TM. Acta Biologica Marisiensis 3(2), 10–21. https://doi.org/10.2478/abmj-2020-0007

Lemenkova P. 2020b. Hyperspectral Vegetation Indices Calculated by Qgis Using Landsat Tm Image: A Case Study of Northern Iceland. Advanced Research in Life Sciences, 4(1), 70–78. https://doi.org/10.2478/arls-2020-0021

Lemenkova P. 2020c. R Libraries {dendextend} and {magrittr} and Clustering Package scipy. Cluster of Python for Modelling Diagrams of Dendrogram Trees. Carpathian Journal of Electronic and Computer Engineering, 13(1), 5–12. https://doi.org/10.2478/cjece-2020-0002

Lemenkova P. 2020d. Sentinel-2 for High Resolution Mapping of Slope-Based Vegetation Indices Using Machine Learning by SAGA GIS. Transylvanian Review of Systematical and Ecological Research, 22(3), 17–34. https://doi.org/10.2478/trser-2020-0015

Lemenkova P. 2021a. SAGA GIS for Computing Multispectral Vegetation Indices by Landsat TM for Mapping Vegetation Greenness. Contemporary Agriculture, 70(1–2), 67–75. https://doi.org/10.2478/contagri-2021-0011

Lemenkova P. 2021b. Dataset compilation by GRASS GIS for thematic mapping of Antarctica: Topographic surface, ice thickness, subglacial bed elevation and sediment thickness. Czech Polar Reports, 1 (1), 67–85. https://doi.org/10.5817/CPR2021-1-6

Li C., Li H., Li J., Lei Y., Li C., Manevski K., Shen Y. 2019. Using NDVI percentiles to monitor real-time crop growth. Computers and Electronics in Agriculture, 162, 357–363. https://doi.org/10.1016/j.compag.2019.04.026

Li R., Liu J. 2004. Estimating wetland vegetation biomass in the Poyang Lake of central China from Landsat ETM data. IGARSS 2004. 2004 IEEE International Geoscience and Remote Sensing Symposium, 7, 4590–4593. https://doi.org/10.1109/IGARSS.2004.1370177

Lv H., Wang Y., Yang Y. 2017. Thin cloud detection using spectral similarity in coastal and blue bands of Landsat-8 data. 2017 IEEE International Geoscience and Remote Sensing Symposium (IGARSS), 2017, 4677–4680. https://doi.org/10.1109/IGARSS.2017.8128045

Mccloy K.R. 2006. Resource Management Information Systems: Remote Sensing, GIS and Modelling. 2nd ed., CRC Taylor & Francis.

Mendenhall C.D., Karp D.S., Meyer C.F.J., Hadly E.A., Daily G.C. 2014. Predicting biodiversity change and averting collapse in agricultural landscapes. Nature, 509, 213–217. https://doi.org/10.1038/nature13139

Mroz M., Sobieraj A. 2004. Comparison of Several Vegetation Indices Calculated on the Basis of a Seasonal Spot XS Time Series, and their Suitability for Land Cover and Agricultural Crop Identification. Technical Sciences, 7, 39–66.

Nagendra H., Lucas R., Honrado J.P., Jongman R.H.G., Tarantino C., Adamo M., Mairota P. 2013. Remote sensing for conservation monitoring: Assessing protected areas, habitat extent, habitat condition, species diversity, and threats. Ecological Indicators, 33, 45–59. https://doi.org/10.1016/j.ecolind.2012.09.014

Olson D., Chatterjee A., Franzen D.W., Day S.S. 2019. Relationship of Drone-Based Vegetation Indices with Corn and Sugarbeet Yields. Agronomy Journal, 111, 2545–2557. https://doi.org/10.2134/agronj2019.04.0260

Onishi M., Ise T. 2021. Explainable identification and mapping of trees using UAV RGB image and deep learning. Scientific Reports, 11, 903. https://doi.org/10.1038/s41598-020-79653-9

Pabi O., Adu-Asare A., Ofori B.D. 2020. Linking Optical SPOT and Unmanned Aerial Vehicle data for a rapid biomass estimation in a Forest-savanna Transitional Zone of Ghana. West African Journal of Applied Ecology, 28(1), 1–20.

Peng B., Guan K., Tang J., Ainsworth E.A., Asseng S., Bernacchi C.J., Cooper M., Delucia E.H., Elliott J.W., Ewert F., Grant R.F., Gustafson D.I., Hammer G.L., Jin Z., Jones J.W., Kimm H., Lawrence D.M., Li Y., Lombardozzi D.L., Marshall-Colon A., Messina C.D., Ort D.R., Schnable J.C., Vallejos C.E., Wu A., Yin X., Zhou W. 2020. Towards a multiscale crop modelling framework for climate change adaptation assessment. Nature Plants, 6, 338–348. https://doi.org/10.1038/s41477-020-0625-3

Pradeep Kumar B., Raghu Babu K., Ramachandra M., Krupavathi C., Narayana Swamy B., Sreenivasulu Y., Rajasekhar M. 2020. Data on identification of desertified regions in Anantapur district, Southern India by NDVI approach using remote sensing and GIS. Data in Brief, 30, 105560. https://doi.org/10.1016/j.dib.2020.105560

Qi J., Chehbouni A., Huete A.R., Kerr Y.H., Sorooshian S. 1994. A modified soil adjusted vegetation index. Remote Sensing of Environment, 48, 119–126. https://doi.org/10.1016/0034-4257(94)90134-1

Rappaport D.I., Royle J.A., Morton D.C. 2020. Acoustic space occupancy: Combining eco acoustics and lidar to model biodiversity variation and detection bias across heterogeneous landscapes. Ecological Indicators, 113, 106172. https://doi.org/10.1016/j.ecolind.2020.106172

Richards J.A. 1986. Remote Sensing Digital Image Analysis: An Introduction. Springer-Verlag, Berlin.

Rondeaux G., Steven M., Baret F. 1996. Optimization of soil-adjusted vegetation indices. Remote Sensing of Environment, 55, 95–107. https://doi.org/10.1016/0034-4257(95)00186-7

Rubin J. 1967. Optimal classification into groups: an approach for solving the taxonomy problem. Journal of Theoretical Biology, 15, 103–144.

Schenke H.W., Lemenkova P. 2008. Zur Frage der Meeresboden-Kartographie: Die Nutzung von AutoTrace Digitizer für die Vektorisierung der Bathymetrischen Daten in der Petschora-See. Hydrographische Nachrichten, 81, 16–21. https://doi.org/10.6084/m9.figshare.7435538

Silleos N.G., Alexandridis T.K., Gitas I.Z., Perakis K. 2006. Vegetation Indices: Advances Made in Biomass Estimation and Vegetation Monitoring in the Last 30 Years. Geocarto International, 21(4), 21–28. https://doi.org/10.1080/10106040608542399

Somvanshi S.S., Kumari M. 2020. Comparative analysis of different vegetation indices with respect to atmospheric particulate pollution using sentinel data. Applied Computing and Geosciences, 7, 100032. https://doi.org/10.1016/j.acags.2020.100032

Suetova I.A., Ushakova L.A., Lemenkova P. 2005. Geoinformation mapping of the Barents and Pechora Seas. Geography and Natural Resources, 4, 138–142. https://doi.org/10.6084/m9.figshare.7435535

Suetova I.A., Ushakova L.A., Lemenkova P. 2005. Geoecological Mapping of the Barents Sea Using GIS. International Cartographic Conference (ICC), La Coruna, Spain. https://doi.org/10.6084/m9.figshare.7435529

Suomalainen J., Oliveira R.A., Hakala T., Koivumäki N., Markelin L., Näsi R., Honkavaara E. 2021. Direct reflectance transformation methodology for drone-based hyperspectral imaging. Remote Sensing of Environment, 266, 1, 112691. https://doi.org/10.1016/j.rse.2021.112691

Suriga S., Hashimoto M., Hoshino B., Saixialt, Ganzorig S. 2012. Change detection method for pasture degradation using RGB color composite image of multitemporal Landsat TM. A case study of the Inner Mongolian settlement region. 2012 IEEE International Geoscience and Remote Sensing Symposium, 2012, 6267–6270. https://doi.org/10.1109/IGARSS.2012.6352691

Taufik A., Ahmad S.S.S., Ahmad A. 2016. Classification of Landsat 8 satellite data using NDVI thresholds. Journal of Telecomunication Electronic and Computer Engineering, 8(4), 37–40.

Teganya Y., Romero D. 2020. Data-Driven Spectrum Cartography via Deep Completion Autoencoders. ICC 2020 – 2020 IEEE International Conference on Communications (ICC), 1–7. https://doi.org/10.1109/ICC40277.2020.9149400

Tripathi M.K., Govil H. 2019. Evaluation of analogical analysis techniques in interpretation of lineaments and litho-boundaries using Landsat 7 ETM+ imagery of western Jahajpur belt, Bhilwara, Rajasthan, India. 2019 4th International Conference on Information Systems and Computer Networks (ISCON), 2019, 213–217. https://doi.org/10.1109/ISCON47742.2019.9036196

Walter-Shea E.A., Privette J., Cornell D., Mesarch M.A., Hays C.J. 1997. Relations between directional spectral vegetation indices and leaf area and absorbed radiation in Alfalfa. Remote Sensing of Environment, 61, 162–177. https://doi.org/10.1016/S0034-4257(96)00250-7

Weiss M., Jacob F., Duveiller G. 2020. Remote sensing for agricultural applications: A meta-review. Remote Sensing of Environment, 236, 111402. https://doi.org/10.1016/j.rse.2019.111402

Westinga E., Beltrana A.P.R., De Bie C.A.J.M., Van Gils H.A.M.J. 2020. A novel approach to optimize hierarchical vegetation mapping from hyper temporal NDVI imagery, demonstrated at national level for Namibia. International Journal of Applied Earth Observation and Geoinformation, 91, 102152. https://doi.org/10.1016/j.jag.2020.102152

Wilson S., Mitchell G.W., Pasher J. et al. 2017. Influence of crop type, heterogeneity and woody structure on avian biodiversity in agricultural landscapes. Ecological Indicators, 83, 218–226. https://doi.org/10.1016/j.ecolind.2017.07.059

Xie Y., Sha Z., Yu M. 2008. Remote sensing imagery in vegetation mapping: a review. Journal of Plant Ecology, 1(1), 9–23. https://doi.org/10.1093/jpe/rtm005

Xu R., Wunsch D.C. 2005. Survey of clustering algorithms. IEEE Transactions on Neural Networks and Learning Systems, 16(3), 645–678. https://doi.org/10.1109/TNN.2005.845141

Yagci A.L., Di L., Deng M. 2014. The influence of land cover-related changes on the NDVI-based satellite agricultural drought indices. 2014 IEEE Geoscience and Remote Sensing Symposium, 2014, 2054–2057. https://doi.org/10.1109/IGARSS.2014.6946868

Yan Y., Jarvie S., Zhang Q., Zhang S., Han P., Liu Q., Liu P. 2021. Small patches are hotspots for biodiversity conservation in fragmented landscapes. Ecological Indicators, 130, 108086. https://doi.org/10.1016/j.ecolind.2021.108086

Yang M., Liu T., Wang X., Yan Y., Hu R., Zhu Q. 2017. Design of WebGIS System Based on Javascript and ArcGIS Server. International Conference on Smart Grid and Electrical Automation (ICSGEA), 709–712. https://doi.org/10.1109/ICSGEA.2017.68

Yang B., Xu Y. 2021. Applications of deep-learning approaches in horticultural research: a review. Horticulture Research, 8, 123. https://doi.org/10.1038/s41438-021-00560-9

Zhang S., Liu L., Liu X., Liu Z. 2016. Development of a new BRDF-Resistant vegetation index for improving the estimation of leaf area index. Remote Sensing, 8, 947.

Zhang H., Ma J., Chen C., Tian X. 2020. NDVI-Net: A fusion network for generating high-resolution normalized difference vegetation index in remote sensing. ISPRS Journal of Photogrammetry and Remote Sensing, 168, 182–196.

Zhi Z., Yin H., Lu N., Zhang X., Yu K., Guo X., Qi H. 2019. Spatial-Temporal Changes of Vegetation Restoration in Yan'an Based on MODIS NDVI and Landsat NDVI. 2019 IEEE International Conference on Signal, Information and Data Processing (ICSIDP), p1-5. https://doi.org/10.1109/ICSIDP47821.2019.9173313

Polina Lemenkova
Université Libre de Bruxelles (ULB),
École polytechnique de Bruxelles (Brussels Faculty of Engineering),
Laboratory of Image Synthesis and Analysis. Building L,
Campus de Solbosch, Avenue Franklin Roosevelt 50, Brussels 1000, Belgium
e-mails: polina.lemenkova@ulb.be
ORCID: 0000-0002-5759-1089